AGU PUBLICATIONS

Geophysical Research Letters

RESEARCH LETTER
10.1002/2017GL075270

Key Points:
- We show the first simulated global dissolved organic carbon (DOC) distribution
- The model captures the measured DOC concentrations with $r = 0.63$ and a bias of 35% despite imperfect temporal matching
- The global average carbon oxidation state (OSc) is shown for both atmospheric and dissolved organic carbon as a metric to describe chemical composition

Correspondence to:
S. A. Safieddine,
sarahsaf@mit.edu

Citation:
Safieddine, S. A., & Heald, C. L. (2017). A global assessment of dissolved organic carbon in precipitation. *Geophysical Research Letters*, *44*, 11,672–11,681. https://doi.org/10.1002/2017GL075270

Received 10 AUG 2017
Accepted 5 NOV 2017
Accepted article online 8 NOV 2017
Published online 27 NOV 2017

A Global Assessment of Dissolved Organic Carbon in Precipitation

Sarah A. Safieddine[1] **and Colette L. Heald**[1]

[1]Department of Civil and Environmental Engineering, Massachusetts Institute of Technology, Cambridge, MA, USA

Abstract Precipitation is the largest physical removal pathway of atmospheric reactive organic carbon in the form of dissolved organic carbon (DOC). We present the first global DOC distribution simulated with a global model. A total of 85 and 188 Tg C yr^{-1} are deposited to the ocean and the land, respectively, with DOC ranging between 0.1 and 10 mg C L^{-1} in this GEOS-Chem simulation. We compare the 2010 simulated DOC to a 30 year synthesis of measurements. Despite limited measurements and imperfect temporal matching, the model is able to reproduce much of the spatial variability of DOC ($r = 0.63$), with a low bias of 35%. We present the global average carbon oxidation state ($\overline{OS_c}$) as a simple metric for describing the chemical composition. In the atmosphere, $-1.8 \leq \overline{OS_c} \leq -0.6$, and the increase in solubility upon oxidation leads to a global increase in $\overline{OS_c}$ in precipitation with $-0.6 \leq \overline{OS_{c\,DOC}} \leq 0$.

1. Introduction

Atmospheric reactive organic carbon (ROC) is central to tropospheric chemistry not only leading to ozone and organic aerosol formation but also providing a large secondary source of carbon dioxide (CO_2). ROC is the sum of atmospheric nonmethane volatile organic compounds and primary and secondary organic aerosol (OA). Chemical transformations, emissions, and physical deposition processes shape the composition and lifecycle of ROC. Physical removal of ROC includes wet and dry deposition processes. Wet deposition describes the scavenging of soluble gases and aerosol particles from the atmosphere by precipitation. Improving the understanding of the composition and evolution of dissolved organic carbon (DOC) in precipitation may therefore provide constraints on the largest physical removal of ROC (Kanakidou et al., 2012; Safieddine et al., 2017), and therefore on its lifecycle.

Wet deposition of species includes in-cloud gas scavenging in liquid water based on Henry's law equilibrium concentrations in rain and snow, gas release by evaporation of rain and snow, and washout of gases by rain and snow falling through air outside clouds (Seinfeld & Pandis, 2006). Meteorological models generally distinguish between two types of precipitation: convective precipitation resulting from convective updrafts and large-scale precipitation resulting from frontal systems or other meteorological processes. Global precipitation is dominated by the latter, particularly outside of the tropics.

As DOC is a ubiquitous component of global precipitation, the atmosphere can be a source of anthropogenic compounds and contaminants to bodies of water near emission sources and can extend to large lakes and the open ocean (Leister & Baker, 1994). DOC can also influence rainwater pH (Willey et al., 2006), cloud albedo (Facchini et al., 1999), and the nutrient enrichment in ecosystems (Seitzinger & Sanders, 1999). The transfer of organic material from the atmosphere to the marine and terrestrial biosphere may therefore impact the environmental health of air, soil, and water.

Little is known about the global magnitude of wet deposition of DOC as a sink of both gas and particle phase reactive organic carbon. DOC concentrations reported in precipitation samples range from 0.2 to 11.4 mg C L^{-1} (Iavorivska et al., 2016). However, measurements are scarce with little to no long-term constraints. As a result, few studies have assessed the wet deposition of DOC. The study by Willey et al. (2000) based on an analysis of sparse global observations suggests a global rainwater deposition flux of 430 ± 150 Tg C yr^{-1}. A modeling study by Kanakidou et al. (2012) looking at organic nitrogen and phosphorus flux into the ocean suggested a total organic flux of 315 Tg C yr^{-1}. Safieddine et al. (2017), using the same model version as in this study, simulated the total budget of reactive organic carbon and suggested a total global wet deposition flux of 273 Tg C yr^{-1}. No previous global assessment of the composition and global distribution of DOC has been presented to date. Here we investigate the simulated DOC composition, spatial distribution, and evolution in the global atmosphere and compare these with historical DOC measurements.

2. Materials and Methods

2.1. Chemical Transport Model

We use the global chemical transport model GEOS-Chem v9-02 (www.geos-chem.org), with modifications as described by Safieddine et al. (2017) to describe atmospheric ROC. In short, the modifications include an expansion of the standard simulation by including new anthropogenic, biomass, biogenic, and ocean emissions, and gas-phase chemistry of aromatics and monoterpenes; an expansion of dry and wet removal treatment; and a complete mass tracking of all reactive carbon species to achieve carbon closure. Secondary organic aerosol (SOA) formation from biogenic and aromatic compounds is described by a volatility basis set scheme, where aerosol is reversibly formed from the first- or second-generation oxidation products of the parent hydrocarbon (Pye et al., 2010) and is coupled to the gas-phase chemical mechanism (Safieddine et al., 2017). Chemical composition of organic species used in this study is based on exact chemical formulae or on the compilation provided by Chen et al. (2015), detailed in the supporting information.

GEOS-Chem is driven by assimilated meteorology from the NASA Global Modeling and Assimilation Office. Our simulations employ GEOS-5.2.0 meteorological data for 2006–2010 at a horizontal resolution of 2° latitude by 2.5° longitude and 47 vertical levels. We use primary organic aerosol anthropogenic emissions from Bond et al. (2007), with emission seasonality from Park (2003) for North America. Global anthropogenic/biofuel emissions are from Emission Database for Global Atmospheric Research (EDGAR-v3) for CO, NO_x, and SO_x and from REanalysis of the TROpospheric chemical composition (RETRO) for VOCs, except ethane emissions (Xiao et al., 2008). Regional emission inventories override the global inventories. These are the Environmental Protection Agency/National Emissions Inventory-2005 for the United States (EPA/NEI, http://www.epa.gov/ttnchie1/trends/), the Criteria Air Contaminants for Canada (CAC, ec.gc.ca/inrp-npri/), Big Bend Regional Aerosol and Visibility Observational Study for Mexico (BRAVO, Kuhns et al., 2005), and Streets et al. (2006) for Asia. Biogenic VOC emissions are calculated interactively within the GEOS-Chem model using the Modern Era Retrospective-Analysis for Research and Applications (MERRA) meteorology based on the Model of Emissions of Gases and Aerosols from Nature (MEGAN) v2.02 (Guenther et al., 2006). Global year-specific biomass-burning emissions are from the Global Fire Emissions Database GFED-3 inventory (Mu et al., 2011).

Removal of gases and particles occurs via wet and dry deposition. Dry deposition is based on a resistance parameterization described by Wesely (1989). Wet scavenging is described by Amos et al. (2012) for gases and Liu et al. (2001) for aerosols. In GEOS-Chem, precipitation is divided between large-scale and convective precipitation. GEOS-5.2.0 data compare well with the Global Precipitation Climatology Project monthly precipitation data set for 2010, which combines observations and satellite precipitation data; the global mean bias is less than 0.2 mm (~1% relative error) with local differences that do not exceed 5 mm (see the supporting information). In this work, Henry's law constants for intermediate species and for species not included in the standard GEOS-Chem chemical mechanism are from Sander (2015, and references therein) and can be found in the supporting information of Safieddine et al. (2017). We note that this version of the GEOS-Chem model does not include scavenging of water-soluble aerosol from cold clouds by homogeneous freezing (Wang et al., 2014); the contribution of this pathway to DOC concentrations is expected to be negligible.

The resulting simulation of the ROC lifecycle is described in Safieddine et al. (2017); here we focus on the removal of organics in precipitation. Previous GEOS-Chem model evaluations of wet removal of chemical species against observation show an average correlation coefficient r = 0.75 (normalized mean bias (NMB) = −5%) for mercury (Amos et al., 2012) r = 0.7 (NMB = −13%), and r = 0.6 (NMB = −15%) for sulfate and ammonium (Fisher et al., 2011), and a NMB of −13% and 11% for ^{210}Pb and ^{7}Be (Liu et al., 2001).

2.2. DOC Measurements

In this study we use the Iavorivska et al. (2016) compilation of observed dissolved organic carbon for the period of 1979–2014. We compare these measurements with our 2010 DOC simulation by interpolating the observation in space and time to monthly averaged GEOS-Chem simulation output for 2010. We discard studies of hurricanes and tropical storms, as these will not be well-represented by the year 2010 meteorology, as well studies with less than 10 DOC samples per year, except marine samples due to their scarcity and less pronounced seasonal variation. As a result, a total of 59 data points (52 after regridding, as different studies over the years occurred in the same location) are used. Different sampling techniques were employed to collect these

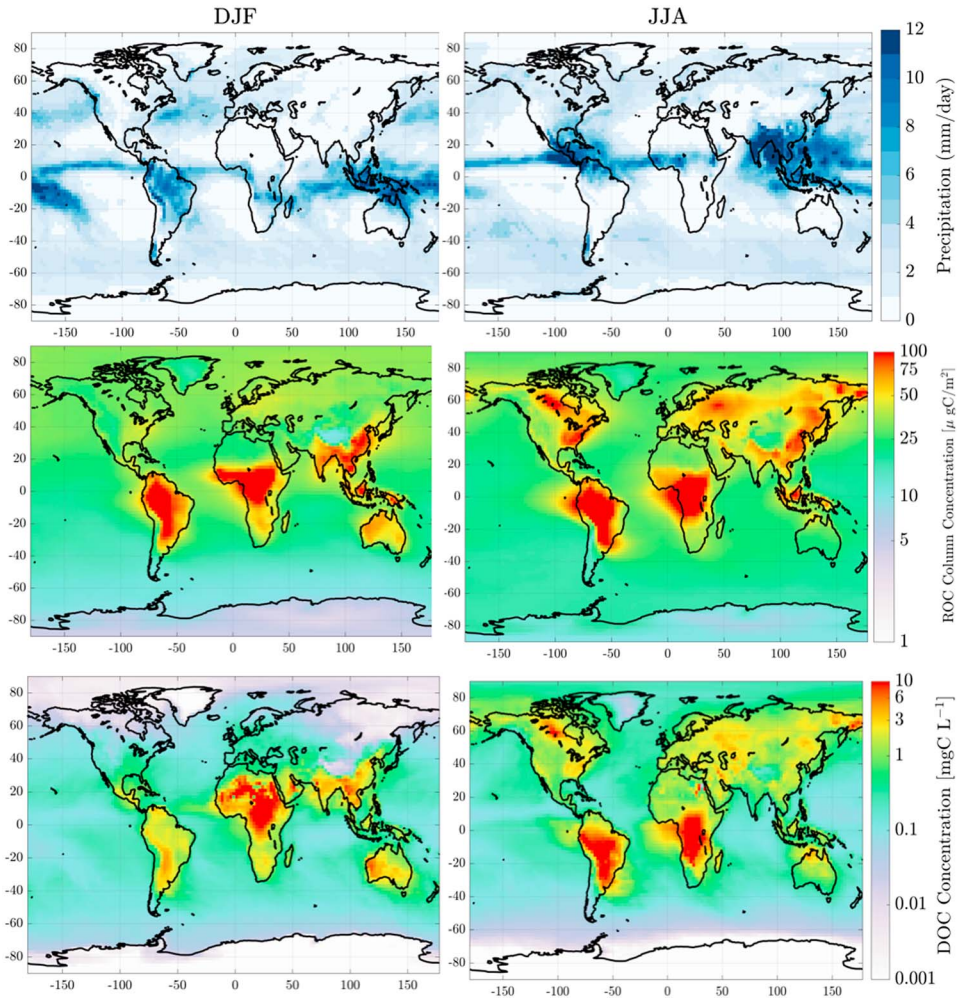

Figure 1. (top to bottom) Average seasonal (DJF: December, January, February and JJA: June, July, August) distribution of precipitation, reactive organic carbon (ROC) column concentrations, and dissolved organic carbon (DOC) concentrations simulated for 2010.

data. Earlier observations (before 1990) relied on wet chemical or ultraviolet (UV) oxidation of the sample to CO_2, and more recently, elemental analysis was performed with an automated analyzer or high-temperature combustion (HTC) of dried samples (Iavorivska et al., 2016). We note that 7 samples out of the 52 samples are labeled as total organic carbon (TOC = POC + DOC, where POC = particulate organic carbon). POC is operationally defined as insoluble compounds that do not pass through a filter with pore sizes that range from 0.2 to 1.0 μm. In principle, TOC should be larger than DOC; however, we choose to retain these samples, as previous studies have shown that DOC makes up the majority (65 to 99%) of TOC depending on location, emissions, and meteorology (Cerqueira et al., 2010; Economou & Mihalopoulos, 2002; Gioda et al., 2008; Willey et al., 2000). We note that in our simulation, washout of insoluble OA contributes less than 0.05% of the DOC wet deposition flux. Measurement uncertainties are not provided by Iavorivska et al. (2016); however, we note that there are substantial differences in measurement technique and sampling across this data set.

3. Results

3.1. Global DOC and Comparison With Observation

Figure 1 shows the simulated seasonal precipitation, ROC, and DOC concentrations. DOC concentrations depend both on precipitation, shown in Figure 1 (top row), and on soluble ROC. High precipitation is

Table 1
Wet Deposition Flux of GEOS-Chem Species

GEOS-Chem species	Description	Formula	Wet deposition flux (Tg C yr^{-1}]
CH_2O	Formaldehyde	CH_2O	49.2
TSOG3 + TSOA3	Lumped semivolatile gas products of monoterpene + sesquiterpene oxidation with C* = 100 μg m^{-3}		30.1 (gas), 1.4 (aerosol)
POA	Primary OA		24.6
IEPOX	Isoprene dihydroxyepoxide epoxide	$C_5H_{10}O_3$	22.7
ISOG3	Lumped semivolatile gas products of isoprene oxidation with C* = 100 μg m^{-3}		22.5
RIP	Peroxide from RIO2 (named as ISOPOOH in the literature)	$HOCH_2C(OOH)(CH_3)CH = CH_2$	17.7
TSOG2 + TSOA2	Lumped semi-volatile gas products of monoterpene + sesquiterpene oxidation with C* = 10 μg m^{-3}		13.3 (gas), 3.4 (aerosol)
HAC	Hydroxyacetone	$HOCH_2C(O)CH_3$	12.2
GLYC	Glycoaldehyde (hydroxyacetaldehyde)	$HOCH_2CHO$	9.6
ACTA	Acetic acid	$CH_3C(O)OH$	9.2
HCOOH	Formic acid	HCOOH	7.8
MGLY	Methylglyoxal	CH_3COCHO	4.8
MP	Methylhydroperoxide	CH_3OOH	4.5
MOH	Methanol	CH_3OH	4.4
GLYX	Glyoxal	CHOCHO	4.3
ISOG1 + ISOA1	Lumped semivolatile aerosol products of isoprene oxidation with C* = 1 μg m^{-3}		3.9 (gas), 4.3 (aerosol)
TSOA0	Lumped semivolatile aerosol products of monoterpene + sesquiterpene oxidation with C* = 0.1 μg m^{-3}		3.2
MAP	Peroxyacetic acid	$CH_3C(O)OOH$	3.1
TSOG1 + TSOA1	Lumped semivolatile aerosol products of monoterpene + sesquiterpene oxidation with C* = 1 μg m^{-3}		1.6 (gas), 1.9 (aerosol)
MMN	Nitrate from methacrolein + methylvinylketone	$HOCH_2CH(ONO_2)C(=O)CH_3$	1.2
ISOG2	Lumped semivolatile gas products of isoprene oxidation with C* = 10 μg m^{-3}		1.2
All other organics			9.9
Total			272

observed in both seasons in the Intertropical Convergence Zone, the South Pacific convergence zone, and the storm tracks in the North Pacific and Atlantic Oceans. Over continental regions, precipitation typically peaks in local summer. Eighty two out of the 166 organic species contributing to the ROC shown in Figure 1 (middle row) are treated in the wet deposition scheme; others are treated as insoluble. A total of 25 species, listed in Table 1, contribute to ~96% of the total wet deposition flux. More information about the budget of reactive organic species can be found in Safieddine et al. (2017). The resulting DOC is shown in Figure 1 (bottom row). DOC is dominated by semivolatile products of monoterpene and sesquiterpene oxidation (20%), formaldehyde (18%), isoprene semivolatile OA (12%), and primary OA (9%). At high latitudes, snow dominates, and DOC is $<$0.01 mg C L^{-1}. Over the terrestrial tropics and midlatitudes, similar to ROC, DOC concentrations are highest near biogenic emission sources. In South East Asian summer, freshly emitted ROC species, in particular from anthropogenic activity, are not soluble, and lead to low DOC values, although the amount of precipitation is high. On average, DOC concentrations are between 0.1 and 1 mg C L^{-1} above the oceans, totaling 85 Tg C yr^{-1} total organic wet deposition flux. DOC concentrations are higher inland, ranging between 1 and 10 mg C L^{-1} with 188 Tg C yr^{-1} total terrestrial organic wet deposition flux. These values are slightly lower than the global estimate of wet deposition based on previous observation and modeling studies, which suggest a global wet deposition flux between 306 and 580 Tg C yr^{-1} out of which 30 to 50% is deposited into the oceans (Jurado et al., 2008; Kanakidou et al., 2012; Willey et al., 2000).

Both ROC and DOC concentrations are higher in June, July, and August (JJA) than in December, January, and February (DJF), as the Northern Hemispheric terrestrial emissions are typically higher during the growing season.

To examine the model skill in simulating DOC concentrations, we show in Figure 2 the 2010 simulated DOC along with the observed DOC concentrations from the historical data set described in section 2.2. Simulating the full 35 year observational record to ensure exact meteorological matching is not computationally feasible. Although we are comparing a 2010 simulation with more than 30 years of DOC observations, the observed DOCs agree reasonably well with simulated values. The model demonstrates some skill in capturing the spatial variability in observed DOC (r = 0.63), with a 35% normalized mean bias $\left(\mathrm{NMB} = \frac{1}{N}\left(\sum_{i=1}^{N}\frac{\mathrm{DOC}_{\mathrm{observed}} - \mathrm{DOC}_{\mathrm{simulated}}}{\mathrm{DOC}_{\mathrm{observed}}}\right)\times 100\right)$. Continental data (in squares) correlate best with our

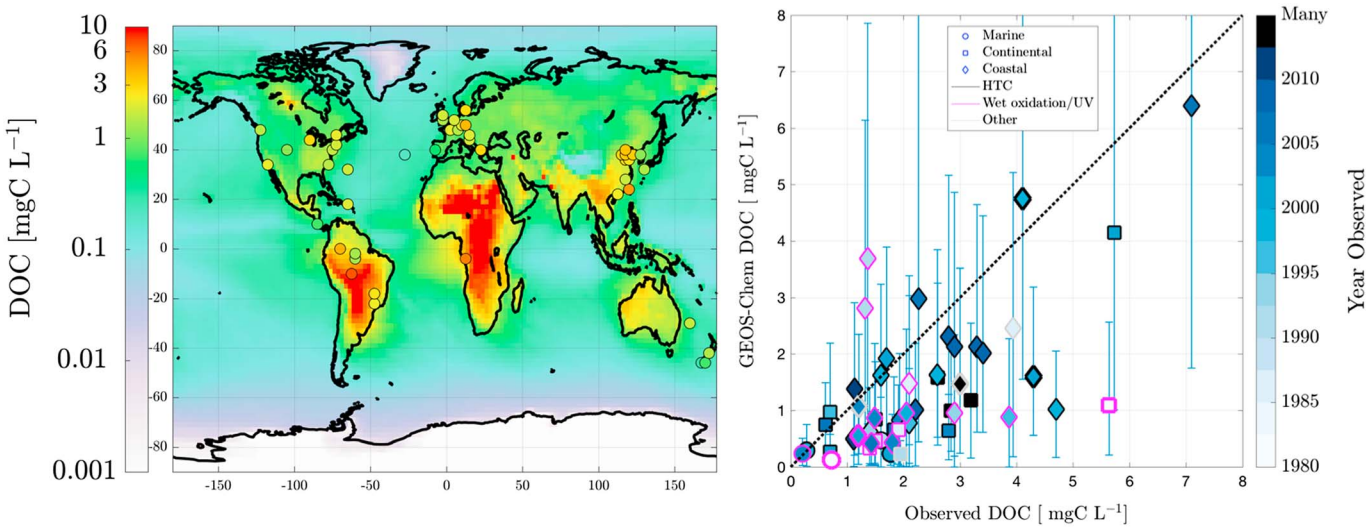

Figure 2. (left) Simulated annual mean (2010) DOC with the location of the historical DOC measurements, in filled circles where the fill color represents the average observed DOC concentrations. (right) Correlation between historical DOC measurements and 2010 simulated volume weighted DOC, sorted by environment (marine, continental, and coastal), and by measurement type (HTC, wet oxidation/UV, or other). The thicker marker lines correspond to TOC measurements (DOC + POC, discussed in section 2.2). Year of measurement is shown with the symbol fill color. The error bars correspond to the minimum and maximum simulated DOC when emissions are fixed to 2010 and meteorology varies between 2006 and 2010.

simulation (R = 0.7), but with the largest bias. The symbol fill colors in Figure 2 (right) indicate the year of observation. It suggests that our simulated DOC for 2010 is more biased when compared to older observations (before 1990). To investigate the potential role of changing anthropogenic emissions on these comparisons, we perform an additional simulation with 2010 meteorology and 1985 and 1990 emissions. While this impacts local concentrations of specific species, we find that the correlation between simulated total DOC and observations is unchanged, and the bias decreases by less than 2%. This suggests that the trend in anthropogenic emissions does not play a substantial role in the model-measurement comparison. Alternatively, this difference may reflect a shift in observational techniques, with HTC measurements (black outlines) being more prevalent in the later part of the record, where agreement between observations and simulation is best. However, comparison between UV/wet oxidation and HTC techniques in the literature show that both methods are comparable (Wallace et al., 2002). Our simulated DOC seems to underestimate, on average, the TOC measurements that include POC in Figure 2. Removing these TOC measurements slightly improves the correlation (r = 0.67, 34% bias).

To investigate the effect of meteorology on DOC, we fix the emissions to 2010 and simulate the DOC over an additional 4 years (2006–2009). The correlation coefficient between the DOCs simulated in different years and the historical data varies between 0.57 and 0.64, while the bias varies between 24 to 39%. The minimum and maximum simulated DOCs during this 5 year-period are plotted as error bars on Figure 2. This suggests that year-to-year variation in meteorology (and particularly precipitation) is an important factor in controlling DOC concentrations.

Finally, we note that some sources of reactive organic carbon are not included in this simulation as they are highly uncertain and not well constrained, and more details of model uncertainties are found in Safieddine et al. (2017). Those sources include mainly intermediate volatility organic compounds; precursors of secondary organic aerosol, with a potential source of ~50–200 Tg yr^{-1} (Hodzic et al., 2016; Jathar et al., 2011; Shrivastava et al., 2015); and emissions of terpenes from the oceans, estimated to total ~40 Tg C yr^{-1} (Luo & Yu, 2010). Our chemical mechanism also does not represent all of the intermediates in the cascade of oxidative chemistry; concentrations of individual species not represented in our scheme are expected to be low, but the sum of these may not be negligible. It remains highly uncertain and unclear how much DOC is underestimated due to these omissions, particularly with respect to the measurement uncertainties discussed above.

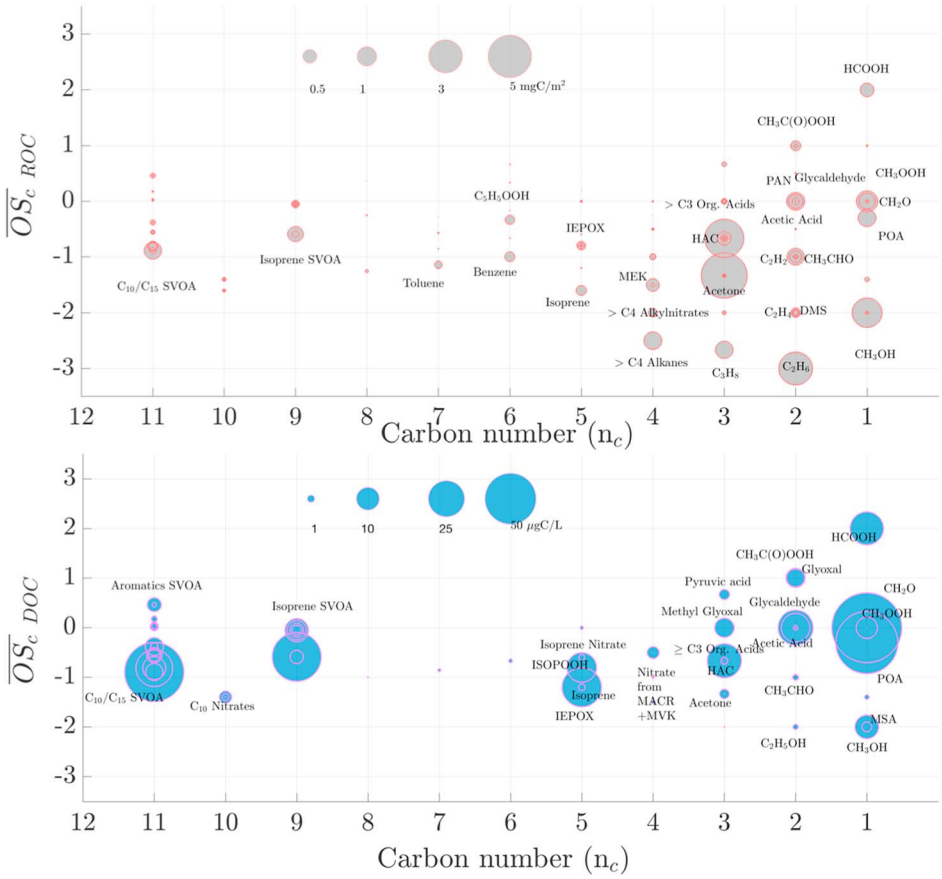

Figure 3. Global mean average (2010) simulated organic carbon composition in the GEOS-Chem model. The carbon oxidation state ($\overline{OS_c}$) versus carbon number (n_c) is shown, weighted by annual mean concentration of the (top) ROC and (bottom) DOC constituents.

The comparison of historical data against the GEOS-Chem model shows that the latter is biased by at most 39%. Factors which likely contribute to this bias include the inexact year-to-year comparison, differences in measurement techniques, omission of certain uncertain sources of ROC in the model, and potential biases in the wet removal scheme. Additional information on the chemical composition of DOC may diagnose the source of this model underestimate and provide insight into the degree of chemical processing of organics in the atmosphere prior to removal.

3.2. Reactive and Dissolved Organic Oxidation State

Organic carbon in the atmosphere and in precipitation is highly complex and poses a significant analytical chemical challenge. A variety of approaches, such as mass spectrometry techniques, attempt instead to provide simplified key information on the chemical composition of organics such as bulk elemental ratios and carbon oxidation state. The average carbon oxidation state $\overline{OS_c} \approx 2\frac{O}{C} - \frac{H}{C}$ (Kroll et al., 2011) is metric for the degree of oxidation of organic species, a quantity that typically increases upon oxidation.

Figure 3 shows the simulated global annual mean ROC and DOC average oxidation state versus carbon number in 2010. The filled circle area is proportional to total carbon mass concentrations. For ROC, the dominant organic species are acetone and hydrocarbons (mainly alkanes and aromatics), organic acids, and alcohols. These have longer lifetimes and can therefore be transported and mixed throughout a hemisphere. Most ROC atmospheric species are relatively reduced, with the alkanes having the lowest $\overline{OS_c}_{\mathrm{ROC}}$. We note that lumping of species in the GEOS-Chem chemical mechanism (e.g., all alkanes ≥ C4 and semivolatile terpene) leads to some ambiguity regarding their molecular weights and carbon number. Here we show these with

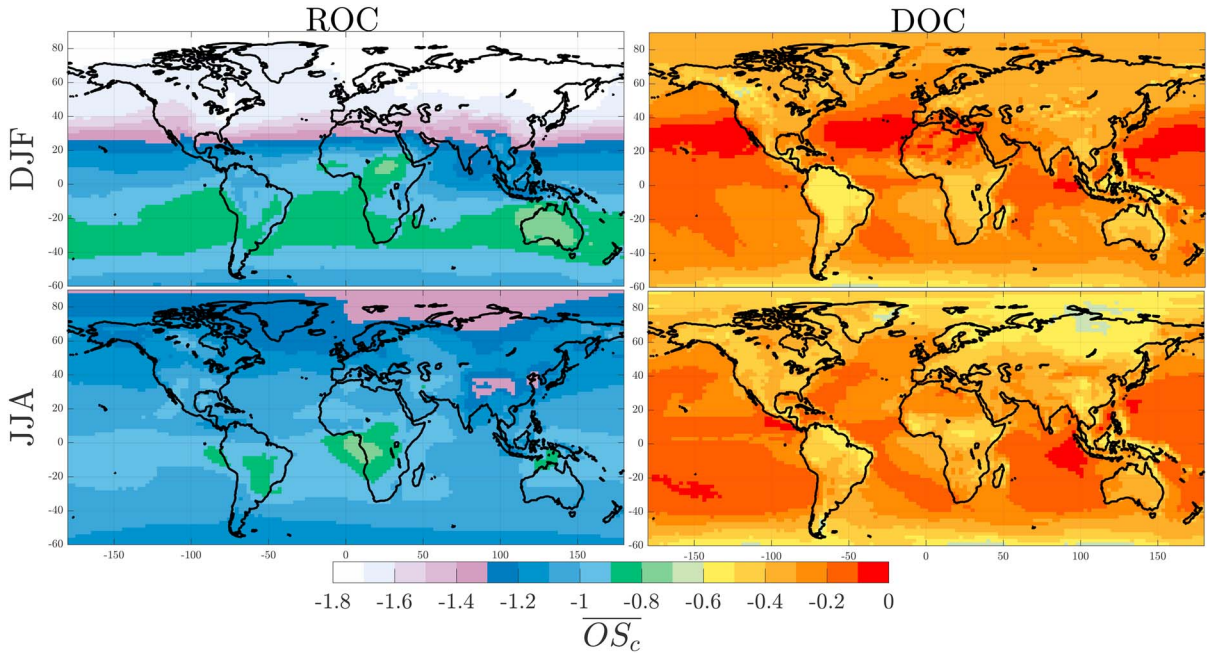

Figure 4. GEOS-Chem simulation of the seasonal mean global mass-weighted carbon oxidation state ($\overline{OS_c}$) of column-integrated (left column) ROC and (right column) DOC in (top row) DJF and (bottom row) JJA.

their lowest carbon number, as shown in Figure 3. This leads to a gap in carbon numbers between 5 and 9, where the only species present are aromatics (benzene, toluene, and xylene) and their oxidation products.

DOC composition depends upon the availability of soluble species. Formaldehyde (CH_2O), primary organic aerosol (POA), secondary semivolatiles, and formic acid (HCOOH) dominate global mean DOC concentrations. POA and aromatic semivolatile aerosols are higher in the Northern Hemisphere (NH), indicative of anthropogenic influence. We note that in the dissolved form, the OA to total DOC mass concentration ratio is a factor of 10 higher than the OA to ROC ratio in the atmosphere since emitted gas-phase biogenic and anthropogenic species, typically the least oxidized and insoluble, dominate ROC. In dissolved form, most of the species have $\overline{OS_{c\,\mathrm{DOC}}} \leq 0$, but higher on average than $\overline{OS_{c\,\mathrm{ROC}}}$. In order to explore the difference between $\overline{OS_{c\,\mathrm{ROC}}}$ and $\overline{OS_{c\,\mathrm{DOC}}}$ globally, we show their mean values spatially in Figure 4.

Globally, the mean mass-weighted carbon oxidation state of ROC and DOC is negative. The $\overline{OS_{c\,\mathrm{ROC}}}$ is between -1.8 and -0.75 but shows clear differences between DJF and JJA. The strong latitudinal gradient seen in DJF is driven by the anthropogenic compounds, emitted in Northern Hemispheric winters, in particular alkanes, as is shown in Figure 3. In JJA, the increase in the $\overline{OS_{c\,\mathrm{ROC}}}$ in the Northern Hemisphere is the result of increased photochemical processing. The Southern Hemisphere shows a small overall decrease between DJF and JJA, and values for both seasons range between -1.8 and -0.75.

In the dissolved form, global $\overline{OS_{c\,\mathrm{DOC}}}$ has less pronounced seasonal and latitudinal variation and is higher in magnitude than the $\overline{OS_{c\,\mathrm{ROC}}}$, with $-0.75 \leq \overline{OS_{c\,\mathrm{DOC}}} \leq 0$. DOC is less sensitive to the seasonality in emissions of anthropogenic compounds, which do not dissolve in rainwater. The global distribution of the $\overline{OS_{c\,\mathrm{DOC}}}$ shows a land/ocean gradient with higher values above oceans. Soluble species over continental regions will undergo oxidation during outflow and transport, leading to an increase in the $\overline{OS_{c\,\mathrm{DOC}}}$ and solubility downwind. The difference in average carbon oxidation state between DOC and ROC can be used to investigate the chemical evolution from ROC to DOC. The largest difference is in the NH winter, reaching 1.5, mainly due to insoluble anthropogenic emission sources, included in ROC but not in DOC. In JJA, we simulate a consistent increase in $\overline{OS_c}$ from ROC to DOC, of 0.3 to 1 over land, and from 0.7 to 1 over the ocean.

Given uncertainties surrounding the formation of SOA in the aqueous phase (aqSOA), we do not include this pathway in our simulation. As atmospheric ROC is dominated by the gas-phase organics, this is unlikely to impact the global mean $\overline{OS_{c\,\mathrm{ROC}}}$. Based on model studies of this source (Fu et al., 2008; Marais et al., 2016),

aqSOA could contribute around 5% of the total simulated wet deposition flux of DOC. The range of the aqSOA $\overline{OS_c}$ found in the literature is 0.04–0.74 (Yu et al., 2014). Therefore, it is likely that aqueous phase production of SOA and the higher $\overline{OS_c}$ of the associated products would also have a very small impact on the $\overline{OS_{c\,\mathrm{DOC}}}$ shown in Figure 4.

While limited observations of rainwater organic composition are currently available, and are often restricted to particular events, e.g., the chemical composition of rainwater throughout Hurricane Irene (Mullaugh et al., 2013), Figure 4 serves as a baseline for comparison with future observations.

4. Conclusions

The removal of atmospheric organic carbon by precipitation prior to its oxidation to carbon dioxide is an important element of the lifecycle of reactive organic carbon in the atmosphere. Assessing this flux also provides constraints on the sources of ROC and the subsequent chemical processing in the atmosphere.

Given the challenges associated with obtaining and archiving precipitation for chemical analysis, the magnitudes of dissolved organic carbon concentration and organic wet deposition flux have been poorly assessed on a global scale. To our knowledge, this is the first study that simulates the global DOC and attempts to compare it with observations. We find a total of 85 Tg C yr^{-1} organic wet deposition flux (DOC < 1 mg C L^{-1}) over the oceans, and higher values inland, ranging between 1 and 10 mg C L^{-1} for DOC and producing a total of 188 Tg C yr^{-1} terrestrial organic wet deposition flux. Our simulated wet deposition flux to the global ocean surface is about 4% of the net annual uptake of ocean CO_2 estimated to be 2.0 ± 1.0 Pg C yr^{-1} in 2000 (Takahashi et al., 2008) and around 43% of the amount of terrestrial particulate organic carbon exported by the rivers to the oceans (Galy et al., 2015). The model is able to capture much of the spatial variability in available historical DOC measurements collected over a period of more than three decades, with a modest low bias. Simulating the DOC over the period of 2006–2010 with fixed 2010 emissions modulates the relative bias from 24 to 39%. This data record covers less than 0.4% of the globe (52 data points, gridded over a 2° × 2.5° grid) over three decades. Our study demonstrates the need for more long-term observational constraints to understand and evaluate the simulated DOC, in particular above remote regions and the open ocean. Challenges in comparing observed against simulated DOC stem from analytical differences in the collected DOC samples and measurements, as well as potential model deficiencies in the simulation of ROC and in its wet removal. In particular, this simulation does not include some ROC sources that are highly uncertain, such as aqueous SOA, intermediate volatility organic compounds, and the emission of terpenes and OA from the oceans. Comparing the chemical composition of both simulated and observed DOC can help identify these deficiencies. We present a metric, the averaged carbon oxidation state $\left(\overline{OSc} \approx 2\frac{O}{C} - \frac{H}{C}\right)$, measured analytically by various instruments that can be used to describe the evolving composition of a complex mixture of organics in the atmosphere and in precipitation. $\overline{OS_c}$ is negative for most of ROC and DOC compounds and is higher in dissolved form due to the increase of solubility upon oxidation. Globally, $-2 \le \overline{OS_{c\,\mathrm{ROC}}} \le -0.75$ and $-0.75 \le \overline{OS_{c\,\mathrm{DOC}}} \le 0$.

This analysis can serve as a reference for future mass spectrometry measurements of DOC. Measurements of the amount and composition of DOC in precipitation offer opportunities to evaluate model representations of the lifecycle of atmospheric ROC and identify critical gaps in our understanding of sources and atmospheric transformations.

Acknowledgments
This work was supported by NOAA (NA14OAR4310132). The authors thank Jesse Kroll for useful discussions and Lidiia Iavorivska for sharing her synthesis of historical DOC data. The GEOS-Chem data used in this study are archived at MIT and available on request from the lead author (sarahsaf@mit.edu).

References

Amos, H. M., Jacob, D. J., Holmes, C. D., Fisher, J. A., Wang, Q., Yantosca, R. M., … Sunderland, E. M. (2012). Gas-particle partitioning of atmospheric Hg(II) and its effect on global mercury deposition. *Atmospheric Chemistry and Physics*, *12*(1), 591–603. https://doi.org/10.5194/acp-12-591-2012

Bond, T. C., Bhardwaj, E., Dong, R., Jogani, R., Jung, S., Roden, C., … Trautmann, N. M. (2007). Historical emissions of black and organic carbon aerosol from energy-related combustion, 1850–2000. *Global Biogeochemical Cycles*, *21*, GB2018. https://doi.org/10.1029/2006GB002840

Cerqueira, M., Pio, C., Legrand, M., Puxbaum, H., Kasper-Giebl, A., Afonso, J., … Fialho, P. (2010). Particulate carbon in precipitation at European background sites. *Journal of Aerosol Science*, *41*(1), 51–61. https://doi.org/10.1016/j.jaerosci.2009.08.002

Chen, Q., Heald, C. L., Jimenez, J. L., Canagaratna, M. R., Zhang, Q., He, L. Y., … Liggio, J. (2015). Elemental composition of organic aerosol: The gap between ambient and laboratory measurements. *Geophysical Research Letters*, *42*, 4182–4189. https://doi.org/10.1002/2015GL063693

Economou, C., & Mihalopoulos, N. (2002). Formaldehyde in the rainwater in the eastern Mediterranean: Occurrence, deposition and contribution to organic carbon budget. *Atmospheric Environment*, *36*(8), 1337–1347. https://doi.org/10.1016/S1352-2310(01)00555-6

Facchini, M. C., Mircea, M., Fuzzi, S., & Charlson, R. J. (1999). Cloud albedo enhancement by surface-active organic solutes in growing droplets. *Nature*, *401*(6750), 257–259. https://doi.org/10.1038/45758

Fisher, J. A., Jacob, D. J., Wang, Q., Bahreini, R., Carouge, C. C., Cubison, M. J., … Yantosca, R. M. (2011). Sources, distribution, and acidity of sulfate–ammonium aerosol in the Arctic in winter–spring. *Atmospheric Environment*, *45*(39), 7301–7318. https://doi.org/10.1016/j.atmosenv.2011.08.030

Fu, T.-M., Jacob, D. J., Wittrock, F., Burrows, J. P., Vrekoussis, M., & Henze, D. K. (2008). Global budgets of atmospheric glyoxal and methylglyoxal, and implications for formation of secondary organic aerosols. *Journal of Geophysical Research*, *113*, D15303. https://doi.org/10.1029/2007JD009505

Galy, V., Peucker-Ehrenbrink, B., & Eglinton, T. (2015). Global carbon export from the terrestrial biosphere controlled by erosion. *Nature*, *521*(7551), 204–207. https://doi.org/10.1038/nature14400

Gioda, A., Mayol-Bracero, O. L., Reyes-Rodriguez, G. J., Santos-Figueroa, G., & Collett, J. L. (2008). Water-soluble organic and nitrogen levels in cloud and rainwater in a background marine environment under influence of different air masses. *Journal of Atmospheric Chemistry*, *61*(2), 85–99. https://doi.org/10.1007/s10874-009-9125-6

Guenther, A., Karl, T., Harley, P., Wiedinmyer, C., Palmer, P. I., & Geron, C. (2006). Estimates of global terrestrial isoprene emissions using MEGAN (Model of Emissions of Gases and Aerosols from Nature). *Atmospheric Chemistry and Physics*, *6*(11), 3181–3210. https://doi.org/10.5194/acp-6-3181-2006

Hodzic, A., Kasibhatla, P. S., Jo, D. S., Cappa, C. D., Jimenez, J. L., Madronich, S., & Park, R. J. (2016). Rethinking the global secondary organic aerosol (SOA) budget: Stronger production, faster removal, shorter lifetime. *Atmospheric Chemistry and Physics*, *16*(12), 7917–7941. https://doi.org/10.5194/acp-16-7917-2016

Iavorivska, L., Boyer, E. W., & DeWalle, D. R. (2016). Atmospheric deposition of organic carbon via precipitation. *Atmospheric Environment*, *146*, 153–163. https://doi.org/10.1016/j.atmosenv.2016.06.006

Jathar, S. H., Farina, S. C., Robinson, A. L., & Adams, P. J. (2011). The influence of semi-volatile and reactive primary emissions on the abundance and properties of global organic aerosol. *Atmospheric Chemistry and Physics*, *11*(15), 7727–7746. https://doi.org/10.5194/acp-11-7727-2011

Jurado, E., Dachs, J., Duarte, C. M., & Simó, R. (2008). Atmospheric deposition of organic and black carbon to the global oceans. *Atmospheric Environment*, *42*(34), 7931–7939. https://doi.org/10.1016/j.atmosenv.2008.07.029

Kanakidou, M., Duce, R. A., Prospero, J. M., Baker, A. R., Benitez-Nelson, C., Dentener, F. J., … Zhu, T. (2012). Atmospheric fluxes of organic N and P to the global ocean. *Global Biogeochemical Cycles*, *26*, GB3026. https://doi.org/10.1029/2011GB004277

Kroll, J. H., Donahue, N. M., Jimenez, J. L., Kessler, S. H., Canagaratna, M. R., Wilson, K. R., … Worsnop, D. R. (2011). Carbon oxidation state as a metric for describing the chemistry of atmospheric organic aerosol. *Nature Chemistry*, *3*(2), 133–139. https://doi.org/10.1038/nchem.948

Kuhns, H., Knipping, E. M., & Vukovich, J. M. (2005). Development of a United States–Mexico Emissions Inventory for the Big Bend Regional Aerosol and Visibility Observational (BRAVO) Study. *Journal of the Air & Waste Management Association*, *55*(5), 677–692. https://doi.org/10.1080/10473289.2005.10464648

Leister, D. L., & Baker, J. E. (1994). Atmospheric deposition of organic contaminants to the chesapeake bay. *Atmospheric Environment*, *28*(8), 1499–1520. https://doi.org/10.1016/1352-2310(94)90210-0

Liu, H., Jacob, D. J., Bey, I., & Yantosca, R. M. (2001). Constraints from 210 Pb and 7 Be on wet deposition and transport in a global three-dimensional chemical tracer model driven by assimilated meteorological fields. *Journal of Geophysical Research*, *106*(D11), 12,109–12,128. https://doi.org/10.1029/2000JD900839

Luo, G., & Yu, F. (2010). A numerical evaluation of global oceanic emissions of α-pinene and isoprene. *Atmospheric Chemistry and Physics*, *10*(4), 2007–2015. https://doi.org/10.5194/acp-10-2007-2010

Marais, E. A., Jacob, D. J., Jimenez, J. L., Campuzano-Jost, P., Day, D. A., Hu, W., … McNeill, V. F. (2016). Aqueous-phase mechanism for secondary organic aerosol formation from isoprene: Application to the southeast United States and co-benefit of SO2 emission controls. *Atmospheric Chemistry and Physics*, *16*(3), 1603–1618. https://doi.org/10.5194/acp-16-1603-2016

Mu, M., Randerson, J. T., van der Werf, G. R., Giglio, L., Kasibhatla, P., Morton, D., … Wennberg, P. O. (2011). Daily and 3-hourly variability in global fire emissions and consequences for atmospheric model predictions of carbon monoxide. *Journal of Geophysical Research*, *116*, D24303. https://doi.org/10.1029/2011JD016245

Mullaugh, K. M., Willey, J. D., Kieber, R. J., Mead, R. N., & Avery, G. B. Jr. (2013). Dynamics of the chemical composition of rainwater throughout Hurricane Irene. *Atmospheric Chemistry and Physics*, *13*(5), 2321–2330. https://doi.org/10.5194/acp-13-2321-2013

Park, R. J. (2003). Sources of carbonaceous aerosols over the United States and implications for natural visibility. *Journal of Geophysical Research*, *108*, 4355. https://doi.org/10.1029/2002JD003190

Pye, H. O. T., Chan, A. W. H., Barkley, M. P., & Seinfeld, J. H. (2010). Global modeling of organic aerosol: The importance of reactive nitrogen (NO_x and NO_3). *Atmospheric Chemistry and Physics*, *10*(22), 11,261–11,276. https://doi.org/10.5194/acp-10-11261-2010

Safieddine, S. A., Heald, C. L., & Henderson, B. H. (2017). The global nonmethane reactive organic carbon budget: A modeling perspective. *Geophysical Research Letters*, *44*, 3897–3906. https://doi.org/10.1002/2017GL072602

Sander, R. (2015). Compilation of Henry's law constants (version 4.0) for water as solvent. *Atmospheric Chemistry and Physics*, *15*(8), 4399–4981. https://doi.org/10.5194/acp-15-4399-2015

Seinfeld, J. H., & Pandis, S. N. (2006). *Atmospheric chemistry and physics from air pollution to climate change* (2nd ed.). New York: John Wiley.

Seitzinger, S. P., & Sanders, R. W. (1999). Atmospheric inputs of dissolved organic nitrogen stimulate estuarine bacteria and phytoplankton. *Limnology and Oceanography*, *44*(3), 721–730. https://doi.org/10.4319/lo.1999.44.3.0721

Shrivastava, M., Easter, R. C., Liu, X., Zelenyuk, A., Singh, B., Zhang, K., … Tiitta, P. (2015). Global transformation and fate of SOA: Implications of low-volatility SOA and gas-phase fragmentation reactions. *Journal of Geophysical Research: Atmospheres*, *120*, 4169–4195. https://doi.org/10.1002/2014JD022563

Streets, D. G., Zhang, Q., Wang, L., He, K., Hao, J., Wu, Y., … Carmichael, G. R. (2006). Revisiting China's CO emissions after the Transport and Chemical Evolution over the Pacific (TRACE-P) mission: Synthesis of inventories, atmospheric modeling, and observations. *Journal of Geophysical Research*, *111*, D14306. https://doi.org/10.1029/2006JD007118

Takahashi, T., Sutherland, S. C., Wanninkhof, R., Sweeney, C., Feely, R. A., Chipman, D. W., … de Baar, H. J. W. (2008). Climatological mean and decadal change in surface ocean pCO_2, and net sea–air CO_2 flux over the global oceans. *Deep Sea Research Part II: Topical Studies in Oceanography*. https://doi.org/10.1016/j.dsr2.2008.12.009

Wallace, B., Purcell, M., & Furlong, J. (2002). Total organic carbon analysis as a precursor to disinfection byproducts in potable water: Oxidation technique considerations. *Journal of Environmental Monitoring*, *4*(1), 35–42. https://doi.org/10.1039/B106049J

Wang, Q., Jacob, D. J., Spackman, J. R., Perring, A. E., Schwarz, J. P., Moteki, N., … Barrett, S. R. H. (2014). Global budget and radiative forcing of black carbon aerosol: Constraints from pole-to-pole (HIPPO) observations across the Pacific. *Journal of Geophysical Research: Atmospheres*, *119*, 195–206. https://doi.org/10.1002/2013JD020824

Wesely, M. L. (1989). Parameterization of surface resistances to gaseous dry deposition in regional-scale numerical models. *Atmospheric Environment*, *23*(6), 1293–1304. https://doi.org/10.1016/0004-6981(89)90153-4

Willey, J. D., Kieber, R. J., & Avery, G. B. (2006). Changing chemical composition of precipitation in Wilmington, North Carolina, U.S.A.: Implications for the continental U.S.A. *Environmental Science & Technology*, *40*(18), 5675–5680. https://doi.org/10.1021/es060638w

Willey, J. D., Kieber, R. J., Eyam, M. S., & Avery, G. B. Jr. (2000). Rainwater dissolved organic carbon: Concentrations and global fluxes. *Global Biogeochemical Cycles*, *14*(1), 139–148. https://doi.org/10.1029/1999GB900036

Xiao, Y., Logan, J. A., Jacob, D. J., Hudman, R. C., Yantosca, R., & Blake, D. R. (2008). Global budget of ethane and regional constraints on U.S. sources. *Journal of Geophysical Research*, *113*, D21306. https://doi.org/10.1029/2007JD009415

Yu, L., Smith, J., Laskin, A., Anastasio, C., Laskin, J., & Zhang, Q. (2014). Chemical characterization of SOA formed from aqueous-phase reactions of phenols with the triplet excited state of carbonyl and hydroxyl radical. *Atmospheric Chemistry and Physics*, *14*(24), 13,801–13,816. https://doi.org/10.5194/acp-14-13801-2014